Regulation of the human thromboxane A_2 receptor gene by Sp1, Egr1, NF-E2, GATA-1, and Ets-1 in megakaryocytes

AnneMarie M. Gannon and B. Therese Kinsella[1]

University College Dublin School of Biomolecular and Biomedical Sciences, University College Dublin Conway Institute of Biomolecular and Biomedical Research, University College Dublin, Belfield, Dublin 4, Ireland

Abstract **The α and β isoforms of the human thromboxane A_2 (TXA_2) receptor (TP) are encoded by a single gene but are transcriptionally regulated by distinct promoters, termed promoter 1 (Prm1) and Prm3, respectively. Herein, it was sought to identify factors regulating Prm1 within the megakaryocytic human erythroleukemia 92.1.7 cell line. Through gene deletion and reporter assays, the core Prm1 was localized to between nucleotides −6,320 and −5,895, proximal to the transcription initiation site. Furthermore, two upstream repressor and two upstream activator regions were identified. Site-directed mutagenesis of four overlapping Sp1/Egr1 elements and an NF-E2/AP1 element within the proximal region substantially reduced Prm1 activity. Deletion/mutation of GATA and Ets elements disrupted the upstream activator sequence located between −7,962 and −7,717, significantly impairing Prm1 activity. Electrophoretic mobility shift assays and chromatin immunoprecipitations confirmed that Sp1, Egr1, and NF-E2 bind to elements within the core promoter, whereas GATA-1 and Ets-1 factors bind to the upstream activator sequence (between −7,962 and −7,717).** **Collectively, these data establish that Sp1, Egr1, and NF-E2 regulate core Prm1 activity in the megakaryocytic-platelet progenitor cells, whereas GATA-1 and Ets-1 act as critical upstream activators, hence providing the first genetic basis for the expression of the human TXA_2 receptor (TP) within the vasculature.**—Gannon, A. M., and B. T. Kinsella. **Regulation of the human thromboxane A_2 receptor gene by Sp1, Egr1, NF-E2, GATA-1, and Ets-1 in megakaryocytes.** ***J. Lipid Res.*** **2008.** 49: **2590–2604.**

Supplementary key words promoter • transcription • prostanoid • platelet

The prostanoid thromboxane A_2 (TXA_2) plays a central role in hemostasis, acting as a potent mediator of platelet aggregation and vasoconstriction (1). Alterations in the levels of the cyclooxygenase 1-derived TXA_2 or of TXA_2 synthase or the TXA_2 receptor (TP) are associated with a variety of vascular disorders, including thrombosis, unstable coronary artery disease, ischemic heart disease, and congestive heart failure (2, 3). Moreover, patients with recent episodes of myocardial infarction or pregnancy-induced hypertension have elevated TP numbers in platelets, suggesting that increased expression of the TP gene in megakaryocytic precursors may underlie the increased tendency toward aggregation or may predispose such individuals to thrombosis (2, 4). Hence, identifying the mechanisms regulating TP gene expression should lead to a greater understanding of its involvement in hemostasis and vascular disease and may provide an increased rationale for intervention approaches.

In humans, TXA_2 actually signals through two TP isoforms, termed TPα and TPβ, that are encoded by a single gene on chromosome 19p13.3 and arise by differential splicing (5). TPα and TPβ are identical in their N-terminal 328-amino-acid residues but differ exclusively in their C-tail domains (5, 6). As members of the G-protein-coupled receptor superfamily, TPα and TPβ show identical coupling to $G\alpha_q$-mediated phospholipase Cβ activation (7), but differentially couple to other secondary effectors, including adenylyl cyclase and tissue transglutaminase (8, 9). TPα and TPβ undergo entirely distinct mechanisms of regulation, such as through agonist-induced homologous (10, 11) and heterologous desensitization (12, 13). For example, TPβ, but not TPα, undergoes tonic and agonist-induced internalization and desensitization through β-arrestin-dependent mechanisms (10, 14). Conversely, TPα, but not TPβ, undergoes desensitization in response to the anti-aggregatory/vasodilatory agents prostacyclin and nitric oxide involving direct phosphorylation of TPα by cAMP- and cGMP-dependent protein kinase, respectively, within its unique C-tail domain (12, 13). The implication from the latter studies is that TPα is the main isoform involved

This work was supported by The Wellcome Trust, The Health Research Board and Science Foundation Ireland.

Manuscript received 16 May 2008 and in revised form 7 July 2008.

Published, JLR Papers in Press, August 12, 2008.
DOI 10.1194/jlr.M800256-JLR200

[1] To whom correspondence should be addressed.
e-mail: Therese.Kinsella@UCD.IE

in hemostasis. Consistent with that hypothesis, although TPα and TPβ also show distinct patterns of mRNA and protein expression in a range of cell and tissue types of vascular origin (15), platelets exclusively express TPα (16).

Hence, although the significance of two receptors for TXA_2 in humans but not in other species is currently unknown, there is abundant and increasing evidence that they have distinct (patho)physiologic roles displaying differences in their signaling, modes of regulation, and patterns of expression. Consistent with this, the TP isoforms are under the transcriptional control of distinct promoters within the single TP gene. Whereas the originally identified promoter (Prm) 1 regulates TPα expression (17), a novel promoter termed Prm3 directs TPβ expression (18). Detailed characterization of Prm3 revealed a central role for both Oct-1/2 and activator protein (AP)-1 in its basal regulation (19).

Despite the recognized importance of TPα, such as in platelets and hemostasis, the factors regulating Prm1 remain largely undefined. Whereas Prm1 is known to lack consensus TATA or CAAT elements (20), transcription initiation is thought to occur at multiple sites within exon 1 of the TP gene (20, 21), and it is suggested that the core promoter may be located within a 500 bp region proximal to the proposed transcription initiation site(s) (22). Considering the central role of TXA_2 in hemostasis and vascular disease, coupled with the lack of detailed knowledge of the factors regulating Prm1 and TPα expression, the central aim of the current study was to characterize Prm1, identifying the *cis*-acting elements and *trans*-acting factors that define both the proximal core promoter and upstream regulatory elements in the platelet progenitor megakaryocytic human erythroleukemia (HEL) 92.1.7 cell line. The data herein categorize Prm1, as distinct from Prm3, as a megakaryocytic promoter under the regulation of both general, including Sp1 and Egr1, and more-specific transcription factors, including NF-E2, GATA-1, and Ets-1.

EXPERIMENTAL PROCEDURES

Materials

pGL3basic and pRL-thymidine kinase (pRL-TK) were obtained from Promega Corporation. DMRIE-C®, RPMI 1640 culture media, and FBS were from Invitrogen Life Technologies. Anti-NF-E2 (sc-291×), anti-Sp1 (sc-59×), anti-Egr1 (sc-110×), anti-WT-1 (sc-192×), anti-cJun (sc-45×), anti-GATA-1 (sc-13053×), anti-Ets-1 (sc-350×), and rabbit IgG (sc-2027) were obtained from Santa Cruz Biotechnology. All antibodies used for chromatin immunoprecipitation (ChIP) analysis were ChIP-validated by the supplier (Santa Cruz Biotechnology) and have been widely used in the literature for such analyses (23–30). The plasmid pCMV-Egr1 was kindly provided by Dr. Gerald Thiel, University of Saarland Medical Centre, Homburg, Germany (31). Bioinformatic analyses to identify putative transcription factor binding sites within Prm1 were carried out using the MatInspector™ program (32).

Construction of luciferase-based genetic reporter plasmids

Prm1 is defined as nucleotides −8,500 to −5,895, located 5′ of the translational ATG initiation codon, designated +1. The plasmid pGL3b:Prm1, containing the Prm1 sequence in the pGL3Basic genetic reporter vector, has been previously described (18). To identify elements required for Prm1 activity, a series of 5′- and 3′-deletion subfragments were subcloned into pGL3Basic. The recombinant plasmids generated, as well as the identities, sequence, and corresponding nucleotides of the specific primers used for each fragment are listed in the expanded Materials and Methods section in the online data supplement at http://www.jlr.org/. The identity and fidelity of all recombinant plasmids were verified by DNA sequence analysis.

Site-directed mutagenesis

Site-directed mutagenesis was carried out using the QuikChange™ method (Stratagene). The identities of the Prm1 elements subjected to site-directed mutagenesis and the corresponding plasmids generated, as well as the identity, sequence, and corresponding nucleotides of the specific primers used are listed in the expanded Materials and Methods section in the online data supplement at http://www.jlr.org/.

Cell culture

HEL 92.1.7 cells, obtained from the American Type Culture Collection, were cultured in RPMI 1640, 10% FBS, at 37°C in a humid environment with 5% CO_2.

Assay of luciferase activity

HEL cells were cotransfected with the various pGL3Basic-recombinant plasmids, encoding firefly luciferase, along with pRL-TK, encoding renilla luciferase, using DMRIE-C® transfection reagent and assayed for firefly and renilla luciferase 48 h later using the Dual-Luciferase Reporter Assay System™ as described (19). Relative firefly to renilla luciferase activities (arbitrary units) were calculated as a ratio and were expressed in relative luciferase units (RLUs).

Western blot analysis

The expression of Sp1, Egr1, NF-E2, GATA-1, and Ets-1 proteins in HEL cells was confirmed by Western blot analysis. Briefly, whole-cell protein was resolved by SDS-PAGE (10% acrylamide gels) and transferred to polyvinylidene difluoride membranes according to standard methodology. Membranes were screened using anti-NF-E2, anti-Sp1, anti-Egr1, anti-GATA-1, or anti-Ets-1 sera in 5% nonfat dried milk in 1× TBS (0.01 M Tris-HCl, 0.1 M NaCl) for 2 h at room temperature, followed by washing and screening using goat anti-rabbit HRP (sc-2204), followed by chemiluminescence detection (13).

Electrophoretic mobility shift and supershift assays

Nuclear extract was prepared from HEL cells as previously described (19). Oligonucleotides corresponding to the sense (5′ end-labeled with biotin) and antisense strands of each probe (90 μM) were annealed by heating at 95°C for 2 min, followed by slow cooling to room temperature. The identities and sequences of the biotin-labeled oligonucleotide probes and the nonlabeled competitor/non-competitor oligonucleotides are listed in the expanded Materials and Methods section in the online data supplement at http://www.jlr.org/.

Initially, serial dilutions of each probe were incubated with nuclear extract (2.5 μg total protein) for 20 min at room temperature in 1× binding buffer [20% glycerol, 5 mM $MgCl_2$, 2.5 mM EDTA (pH 8.0), 250 mM NaCl, 50 mM Tris-HCl (pH 8.0), and 0.25 mg ml^{-1} poly (dI-dC; Sigma)]. Protein-DNA complexes were subjected to electrophoresis through 6% DNA retardation gels (Invitrogen) in Tris borate EDTA buffer for 1–2 h at room tem-

perature and then transferred to Biodyne® B positively charged nylon membrane (Pall). Thereafter, detection was carried out using the Chemiluminescence Nucleic Acid Detection Module (33), as described by the manufacturer. Once the optimal concentration of each probe was determined, binding reactions were set up by incubating nuclear extract (2.5 μg total protein) with/without 300-fold molar excesses of nonlabeled double-stranded competitors/non-competitors in 1× binding buffer for 20 min at room temperature. The appropriate concentration of biotin-labeled probe was then added, and mixtures were incubated for 20 min at room temperature, after which electrophoresis, transfer, and detection were carried out, as before.

For supershift assays, nuclear extract (2.5 μg total protein) was preincubated with 3 μg of anti-NF-E2, anti-Sp1, anti-Egr1, anti-WT-1, or anti-cJun sera for 2 h at 4°C. Thereafter, the nuclear extract-antibody mixtures were incubated for 20 min at room temperature with the appropriate biotin-labeled double-stranded probe, as described in the expanded Materials and Methods section in the online data supplement at http://www.jlr.org/.

ChIP assays

ChIP assays were performed essentially as described (34). Specifically, HEL cells (1×10^8) were pelleted, washed in ice-cold PBS, and resuspended in serum-free RPMI 1640. Formaldehyde-cross-linked chromatin was sonicated, as described (34), to generate fragments 500 bp to 1,000 bp in length. Prior to immunoprecipitation, chromatin was incubated with 60 μg normal rabbit IgG overnight at 4°C on a rotisserie, after which 250 μl of salmon sperm DNA/protein A agarose beads (Millipore) were added, and chromatin was precleared for 3 h at 4°C with rotation. Thereafter, anti-NF-E2, anti-Sp1, anti-Egr1, anti-GATA-1, anti-Ets-1 (10 μg aliquots), or normal rabbit IgG (10 μg) was used for immunoprecipitation. Following elution, cross-links were reversed by incubation at 65°C overnight, followed by protease digestion with proteinase K (Sigma; 9 μl of 10 mg/ml) at 45°C for 7 h. After precipitation, samples were resuspended in 50 μl dH_2O. PCR analysis was carried out using 2–3 μl of ChIP sample as template or, as a positive control, with an equivalent volume of a 1:20 dilution of the input chromatin DNA. The identities of the primers used for the ChIP PCR reactions, as well as their sequences and corresponding nucleotides within Prm1, are listed in the expanded Materials and Methods section in the online data supplement at http://www.jlr.org/.

Statistical analysis

Statistical differences were routinely analyzed using the two-tailed Student's unpaired *t*-test. All values are expressed as mean ± standard error of the mean (SEM). *P* values < 0.05 were considered to indicate statistically significant differences, and *, **, ***, and **** indicate $P < 0.05$, $P < 0.01$, $P < 0.001$, and $P < 0.0001$, respectively.

RESULTS

Functional analysis of Prm1 of the human TXA_2 receptor gene

The aim of this investigation was to characterize Prm1 of the human TXA_2 receptor (TP) gene within the megakaryocytic HEL 92.1.7 cell line, seeking to identify the key factors regulating TPα expression in platelets and related cell types. Prm1 is defined as nucleotides −8,500 to −5,895 upstream of the translational initiation codon (18). A series of 5′ deletions was generated, where the 5′ nucleotide of each subfragment is indicated in brackets throughout. Through genetic reporter assays, the recombinant plasmid pGL3b:Prm1 directed 7.83 ± 0.70 RLUs in HEL cells (**Fig. 1A**), compared with 23.9 ± 1.1 RLUs directed by an SV40 promoter in the pGL3control vector, which acted as a reference. Deletion of Prm1 (−8,500) to Prm1B (−7,962) yielded a 2.8-fold increase in luciferase activity ($P < 0.0001$). Further 5′ deletion to generate Prm1BΔ (−7,717) resulted in a 2.4-fold decrease in luciferase expression ($P < 0.0001$). Moreover, progressive 5′ deletion to generate Prm1C (−7,504) yielded a further 1.8-fold reduction ($P = 0.0014$), whereas deletion of nucleotides from Prm1D (−6,848) to generate Prm1E (−6,648) resulted in a 1.3-fold increase ($P = 0.0242$) in luciferase expression. Hence, 5′ deletion analysis revealed two upstream repressor sequences (URSs) between −8,500 to −7,962 and −6,848 to −6,648 and two upstream activator sequences (UASs) between −7,962 to −7,717 and −7,717 to −7,504 within Prm1. The Prm1E (−6,648) subfragment directed luciferase expression comparable to that of the full-length Prm1, indicating that Prm1E contains core elements required to direct minimal Prm1 activity. Consistent with this, 3′ deletion of nucleotides −6,437 to −5,895 from Prm1BΔ, Prm1C, and Prm1E significantly reduced luciferase expression ($P < 0.0001$ in each case; Fig. 1B), to levels that were not substantially greater than that of pGL3Basic, such as in the case of Prm1E 3′ deletion. These data further suggest that the proximal Prm1E (−6,648) contains the core elements required to direct minimal Prm1 activity.

Identification of functional NF-E2 and overlapping Sp1/Egr1 elements in Prm1

Successive 5′ deletions of Prm1E (−6,648) further localized the positive regulatory element(s) between −6,648 and −5,895 (**Fig. 2A**). Deletion of nucleotides from −6,648 to generate Prm1HΔ (−6,320) did not affect luciferase expression, but generation of Prm1K (−6,067) and Prm1L (−6,010) led to 1.3-fold ($P = 0.0003$) and 1.8-fold ($P < 0.0001$) reductions, respectively.

Further 5′ deletions, to generate Prm1F–1J (data not shown), in combination with bioinformatic analysis to identify elements within the −6,320 to −5,895 region revealed five putative overlapping sites for Sp1/Egr1 and a putative NF-E2/AP1 site (Fig. 2). Hence, site-directed mutagenesis was used to disrupt those putative Sp1/Egr1 and NF-E2/AP1 sites within either Prm1HΔ (−6,320) or Prm1L (−6,010). Mutation of the Sp1/Egr1$^{-6,007}$ site within Prm1L significantly reduced but did not abolish luciferase expression (Fig. 2A, $P = 0.0135$). Mutation of four of the five Sp1/Egr1 sites, specifically Sp1/Egr1$^{-6,294}$, Sp1/Egr1$^{-6,278}$, Sp1/Egr1$^{-6,022}$, and Sp1/Egr1$^{-6,007}$, but not Sp1/Egr1$^{-6,098}$, each reduced luciferase activity directed by Prm1HΔ ($P = 0.0096$, $P = 0.0005$, $P < 0.0001$, and $P < 0.0001$, respectively; Fig. 2B). Furthermore, disruption of the putative NF-E2/AP1$^{-6,080}$ site also reduced luciferase activity directed by Prm1HΔ ($P < 0.0001$).

Thereafter, to investigate possible cooperative actions of the latter, the effect of mutating combinations of the Sp1/Egr1 and NF-E2/AP1 elements within Prm1HΔ was exam-

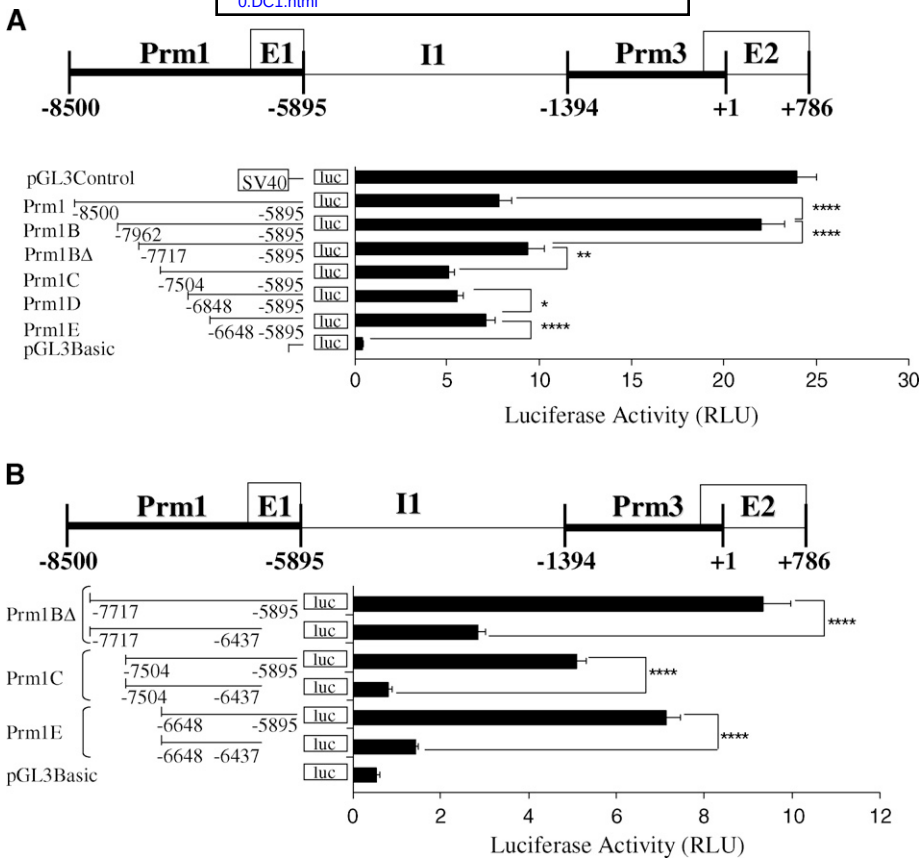

Fig. 1. Effect of 5′ and 3′ deletions on Prm1-directed gene expression. Schematic of the human TP gene spanning nucleotides −8,500 to +786, encoding Prm1 (−8,500 to −5,895), Prm3, exon (E)1, intron (I)1 and E2, where nucleotide +1 represents the translational start site (ATG). Plasmids (2 μg) encoding (A) pGL3control [positive control; 23.9 ± 1.1 relative luciferase units (RLUs)], Prm1, Prm1B, Prm1BΔ, Prm1C, Prm1D, and Prm1E; (B) Prm1BΔ, Prm1BΔ 3′deletion, Prm1C, Prm1C 3′deletion, Prm1E, Prm1E 3′deletion, or, as a negative control, pGL3Basic (A, B) were cotransfected with pRL-TK into HEL 92.1.7 cells. Mean firefly relative to renilla luciferase activity was expressed in arbitrary relative luciferase units (RLU ± SEM; n = 5).

ined (Fig. 2C and data not shown). As stated, disruption of Sp1/Egr1$^{-6,294}$ and disruption of Sp1/Egr1$^{-6,022}$ both decreased luciferase expression directed by Prm1HΔ, where disruption of Sp1/Egr1$^{-6,022}$ caused a more pronounced decrease (1.8-fold; $P < 0.0001$) than mutation of Sp1/Egr1$^{-6,294}$ (1.3-fold; $P = 0.0096$). Mutation of both elements together, generating Prm1HΔ$^{Sp1/Egr1(-6,294,-6,022)*}$, also decreased luciferase expression compared with that of Prm1HΔ ($P < 0.0001$). However, the magnitude of this decrease (1.8-fold) was not greater than that of Sp1/Egr1$^{-6,022}$ alone. Furthermore, the activity directed by Prm1HΔ$^{Sp1/Egr1(-6,294,-6,022)*}$ was not significantly different from that of Prm1HΔ$^{Sp1/Egr1(-6,022)*}$ ($P = 0.5033$). Similarly, mutation of Sp1/Egr1$^{-6,022}$ and Sp1/Egr1$^{-6,007}$ both led to decreased luciferase expression directed by Prm1HΔ (1.8-fold; $P < 0.0001$ and 1.5-fold; $P < 0.0001$, respectively). Disruption of both elements, generating Prm1HΔ$^{Sp1/Egr1(-6,022,-6,007)*}$, reduced luciferase expression relative to that of Prm1HΔ ($P = 0.0001$). The extent of this decrease (1.5-fold) was of the same order as that caused by Sp1/Egr1$^{-6,007}$. Moreover, the luciferase activity directed by Prm1HΔ$^{Sp1/Egr1(-6,022,-6,007)*}$ was not significantly different from that of Prm1HΔ$^{Sp1/Egr1(-6,022)*}$ ($P = 0.1333$) or Prm1HΔ$^{Sp1/Egr1(-6,007)*}$ ($P = 0.7571$). Hence, collectively, these and other combinations of mutations (data not shown) indicate that the Sp1/Egr1 and/or NF-E2/AP1 elements within the −6,320 to −5,895 region act interdependently and functionally cooperate to regulate Prm1.

Thereafter, electrophoretic mobility shift assays (EMSAs) were carried out to investigate the presence and identity of nuclear factors capable of binding to the NF-E2/AP1$^{-6,080}$ element in vitro (**Fig. 3A**). Expression of NF-E2 (Fig. 3C) and the AP1 component cJun (data not shown) in HEL 92.1.7 cells was confirmed by immunoblot analysis. Incubation of a biotin-labeled NF-E2/AP1 probe with nuclear extract from HEL cells resulted in the appearance of a main protein-DNA complex, C1, as well as one or more faster migrating complexes (Fig. 3A, lane 2). The main C1 complex was competed by specific NF-E2/AP1$^{-6,080}$ or consensus NF-E2 sequences but not by a consensus AP1 sequence (Fig. 3A, lanes 3–5). It appears that the faster migrating complexes were competed in a similar manner to C1. Following prolonged exposure of the chromatogram shown in Fig. 3A, a further slower migrating complex, designated

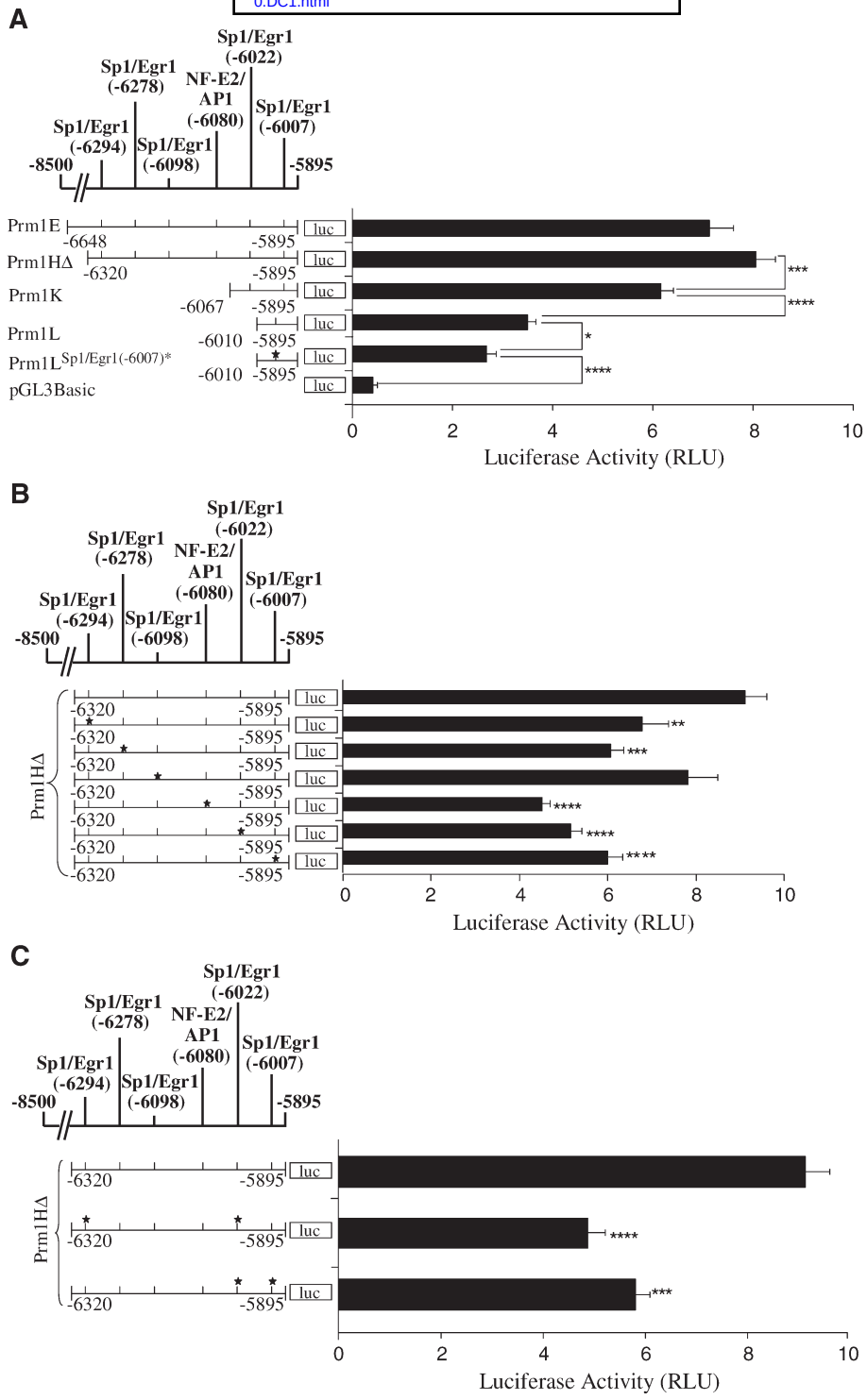

Fig. 2. Identification of NF-E2/AP1 and Sp1/Egr1 elements within Prm1. Putative Sp1/Egr1 and NF-E2/AP1 elements within Prm1, where the 5′ nucleotide is indicated and the star symbol signifies mutated elements. pGL3Basic plasmids (2 μg) encoding (A) Prm1E, Prm1HΔ, Prm1K, Prm1L, Prm1L$^{Sp1/Egr1(-6,007)*}$ and, as a control, pGL3Basic; (B) Prm1HΔ, Prm1HΔ$^{Sp1/Egr1(-6,294)*}$, Prm1HΔ$^{Sp1/Egr1(-6,278)*}$, Prm1HΔ$^{Sp1/Egr1(-6,098)*}$, Prm1HΔ$^{NF\text{-}E2/AP1(-6,080)*}$, Prm1HΔ$^{Sp1/Egr1(-6,022)*}$, and Prm1HΔ$^{Sp1/Egr1(-6,007)*}$; or (C) Prm1HΔ, Prm1HΔ$^{Sp1/Egr1(-6,294,-6,022)*}$, Prm1HΔ$^{Sp1/Egr1(-6,022,-6,007)*}$ were cotransfected with pRL-TK into HEL 92.1.7 cells. Luciferase activity was expressed as mean firefly relative to renilla luciferase activity (RLU ± SEM; n = 5).

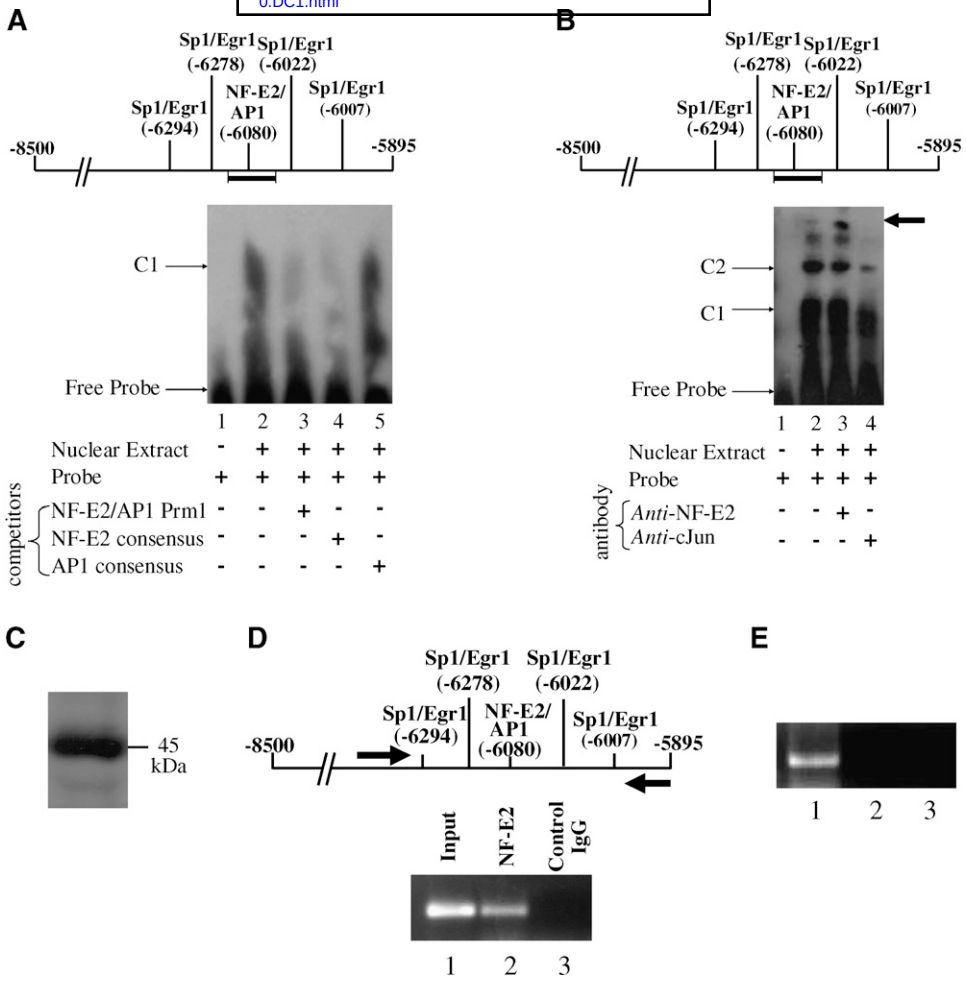

Fig. 3. NF-E2 binding to the proximal Prm1. Electrophoretic mobility shift assays (EMSAs) (A) or supershift assays (B) using nuclear extract from HEL cells and a biotin-labeled double-stranded NF-E2/AP1 probe (Probe) spanning −6,087 to −6,049 of the TP gene, as indicated by the horizontal bar. A: Nuclear extract was preincubated with the vehicle (−) or with excess nonlabeled competitor oligonucleotides (+) prior to addition of the NF-E2/AP1 probe. One main complex, C1, as well as one or more faster migrating complexes, was observed; prolonged exposure revealed a slower migrating C2 complex (not shown). B: Nuclear extract was preincubated with vehicle (−), anti-NF-E2 (+), or anti-cJun (+) sera before addition of the biotinylated NF-E2 probe. Two main complexes, C1 and C2, were observed. The arrow to the right indicates the supershifted transcription factor:DNA complex detected with the anti-NF-E2 serum (lane 3). C: Immunoblot analysis of NF-E2 expression in HEL cells (60 μg whole-cell protein). D, E: Chromatin immunoprecipitation (ChIP) analysis of Prm1. Schematic of Prm1 and primers (arrows) used in the PCR to detect the proximal Prm1 region [−6,368 to −5,895; (D)] from input chromatin or anti-NF-E2 or, as a control, normal rabbit IgG immunoprecipitates of cross-linked chromatin from HEL cells. Primers to detect an upstream region of Prm1 [−8,460 to −8,006; (D)] from input chromatin, anti-NF-E2, or normal rabbit IgG precipitates were used as a negative control. Images are representative of three independent experiments.

C2, and equivalent to C2 shown in Fig. 3B, was observed and, like C1, was competed by NF-E2/AP1$^{-6,080}$ and consensus NF-E2 sequences but not by the consensus AP1 sequence (data not shown). Thereafter, preincubation of nuclear extract with an anti-NF-E2 antibody resulted in a supershifted complex (Fig. 3B). However, it appeared that C1 was not significantly reduced following formation of this supershift, suggesting that the supershifted NF-E2 may have originated from a complex other than C1. Although no supershift was observed with an anti-cJun antibody, it appeared that addition of this antibody reduced both C1 and C2, suggesting a possible role for cJun binding to the NF-E2/AP1 probe (Fig. 3B, lane 4). To investigate whether NF-E2 can directly bind to Prm1 in vivo, ChIP assays were carried out on chromatin extracted from HEL cells (Fig. 3D). PCR analysis using primers specific to the 3′ Prm1 region (−6,368 to −5,895) generated amplicons from both the input chromatin and from an anti-NF-E2, but not from a control IgG immunoprecipitate (Fig. 3D). PCR analysis using primers specific to the −8,460 to −8,006 region of Prm1, which does not contain any predicted NF-E2 elements, resulted in generation of an amplicon from input chromatin, but not from anti-NF-E2 or IgG precipitates (Fig. 3E). Taken together, EMSA and super-

shifts demonstrate that NF-E2 specifically binds to the NF-E2/AP1$^{-6,080}$ probe in vitro, whereas ChIP assays establish that NF-E2 occupies element(s) within the −6,368 to −5,895 region of Prm1 in vivo.

EMSAs also investigated nuclear factor binding to the Sp1/Egr1$^{-6,294}$ and Sp1/Egr1$^{-6,278}$ elements in vitro. Immunoblot analysis confirmed abundant expression of Sp1 and Egr1 in HEL cells (**Fig. 4A, B**). Incubation of the Sp1/Egr1$^{-6,294}$ probe with nuclear extract generated two DNA-protein complexes, C1 and C2 (Fig. 4C, lane 2). Both C1 and C2 were efficiently competed by the Sp1/Egr1$^{-6,294}$ and consensus Egr1 sequences (Fig. 4C, lanes 3 and 5, respectively), and to a lesser extent by consensus Sp1 and WT-1 sequences (Fig. 4C, lanes 4 and 6, respectively). Neither C1 nor C2 were competed by a nonspecific randomized sequence based on the TP gene (Fig. 4C, lane 7). Moreover, addition of an anti-Egr1 antibody resulted in generation of a supershift complex, as well as reducing both C1 and C2 (Fig. 4D, lane 4). Although no supershift was observed with an anti-Sp1 antibody, both C1 and C2 were substantially reduced following its addition (Fig. 4D, lane 3), indicating a possible role for Sp1 binding to the probe. Addition of an anti-WT-1 antibody or an anti-cJun antibody, used as a control, had no substantial effects on binding patterns to the probe (Fig. 4D, lanes 5 and 6, respectively). Collectively, these data indicate that complexes of Sp1 and Egr1 from HEL cell nuclear extract can bind to the Sp1/Egr1$^{-6,294}$ element within Prm1 in vitro.

Thereafter, EMSAs were carried out to investigate the presence of nuclear factors capable of binding to the Sp1/Egr1$^{-6,278}$ element in vitro. Incubation of the Sp1/Egr1$^{-6,278}$ probe with HEL cell nuclear extract generated one main complex, designated C1 (Fig. 4E, lane 2). C1 was efficiently competed by Sp1/Egr1$^{-6,278}$, consensus Sp1, and consensus Egr1 sequences, and to a much lesser extent, by the WT-1 sequence (Fig. 4E, lanes 3–6, respectively). C1 was not competed by a nonspecific randomized sequence based on the TP gene (Fig. 4E, lane 7). Moreover, addition of an anti-Egr1 antibody generated a supershift complex, as well as reducing the main complex, C1 (Fig. 4F, lane 4). Although addition of an anti-Sp1 antibody did not lead to the observation of a supershift complex, it reduced C1 in a manner similar to that of the anti-Egr1 antibody, indicating a possible role for Sp1 binding. Addition of an anti-WT-1 antibody or an anti-cJun antibody, used as a control, did not have any substantial effects on binding patterns to the probe. Collectively, these data indicate that a complex of Sp1 and Egr1 from HEL cell nuclear extract can bind to the Sp1/Egr1$^{-6,278}$ element within Prm1 in vitro.

EMSAs also confirmed the presence of nuclear factors capable of binding to the Sp1/Egr1$^{-6,022}$ and Sp1/Egr1$^{-6,007}$ elements in vitro. Incubation of the Sp1/Egr1$^{-6,022,-6,007}$ probe with HEL cell nuclear extract resulted in two main complexes, C1 and C2 (**Fig. 5A**). Both C1 and C2 were competed by both Sp1/Egr1$^{-6,022}$- and Sp1/Egr1$^{-6,007}$-specific sequences (Fig. 5A, lanes 3–5, respectively). The faster migrating C1 complex was efficiently competed by consensus Sp1, consensus Egr1, and WT-1 sequences (Fig. 5A, lanes 6–8, respectively). It was notable, however, that C2 was actually increased by consensus Sp1, Egr1, or WT-1 oligonucleotides (Fig. 5A, lanes 6–8, respectively), suggesting that nuclear factors other than Sp1, Egr1, or WT-1 may possibly bind to the Sp1/Egr1$^{-6,022,-6,007}$ probe in vitro, and that these factors may bind more efficiently to the probe when the proteins involved in the formation of C1 are unavailable for binding. A nonspecific randomized sequence based on the TP gene (Fig. 5A, lane 9) failed to inhibit C1 or C2. These data indicate that Sp1, Egr1, and/or WT-1 proteins from HEL cells bind to the sites at −6,022 and −6,007 within Prm1. Moreover, anti-Sp1 (Fig. 5B left, lane 3) and anti-Egr1 (Fig. 5B right, lane 4) antibodies both resulted in supershift complexes, whereas no supershifts were observed with either anti-WT-1 or, as a control, anti-cJun antibodies, even following prolonged exposure of the chromatogram (Fig. 5B, lanes 5 and 6, respectively). Due to the weak nature of the supershifted complexes observed following preincubation with either anti-Sp1 or anti-Egr1 antibodies, it was not clear whether the Sp1 or Egr1 in the supershifted complexes actually originated from C1.

Thereafter, to further investigate the possible binding of Sp1 and Egr1 to the proximal Prm1, ChIP analysis was carried out. Primers based on the proximal Prm1 region generated amplicons from both anti-Sp1 and anti-Egr1, but not from the control IgG immunoprecipitates (Fig. 5C). Conversely, PCR analysis using primers specific to an upstream region of Prm1 from −8,460 to −8,006 resulted in generation of an amplicon from input chromatin, but not from anti-Sp1, anti-Egr1, or IgG precipitates (Fig. 5D). Additionally, overexpression of Egr1 led to a modest but significant decrease in the luciferase expression directed by Prm1HΔ in HEL cells (Fig. 5E). Hence, collectively, four overlapping Sp1/Egr1 sites and an NF-E2 site have been identified in the proximal Prm1 region. Both Sp1 and Egr1, in addition to NF-E2, bind to those elements in vitro and in vivo to regulate core Prm1, whereas overexpression of Egr1 appears to negatively regulate that transcriptional activity.

Identification of functional GATA and Ets sites within Prm1

As stated, 5′ deletions of Prm1 revealed a UAS between −7,962 (Prm1B) and −7,717 (Prm1BΔ), deletion of which yielded a 2.8-fold reduction in luciferase expression (Fig. 1A). To localize the regulatory element(s) within this region, an additional 5′ subfragment, Prm1BΔGata/Ets, (−7,859) was generated. Removal of nucleotides between −7,962 (Prm1B) and −7,859 (Prm1BΔGata/Ets) led to a 2.3-fold reduction in luciferase activity (**Fig. 6A**; $P < 0.0001$), whereas there was no difference in expression between Prm1BΔGata/Ets and Prm1BΔ ($P = 0.261$). Among the transcription factor elements identified between −7,962 and −7,859 were putative GATA and Ets elements at −7,890 and −7,870, respectively. Mutation of GATA$^{-7,890}$ and Ets$^{-7,870}$ elements both reduced luciferase expression directed by Prm1B (Fig. 6B), where the decrease due to the Ets$^{-7,870}$ mutation (2.2-fold; $P < 0.0001$) was more pronounced than that caused by the GATA$^{-7,890}$ mutation (1.8-fold; $P < 0.0001$). Luciferase expression directed by

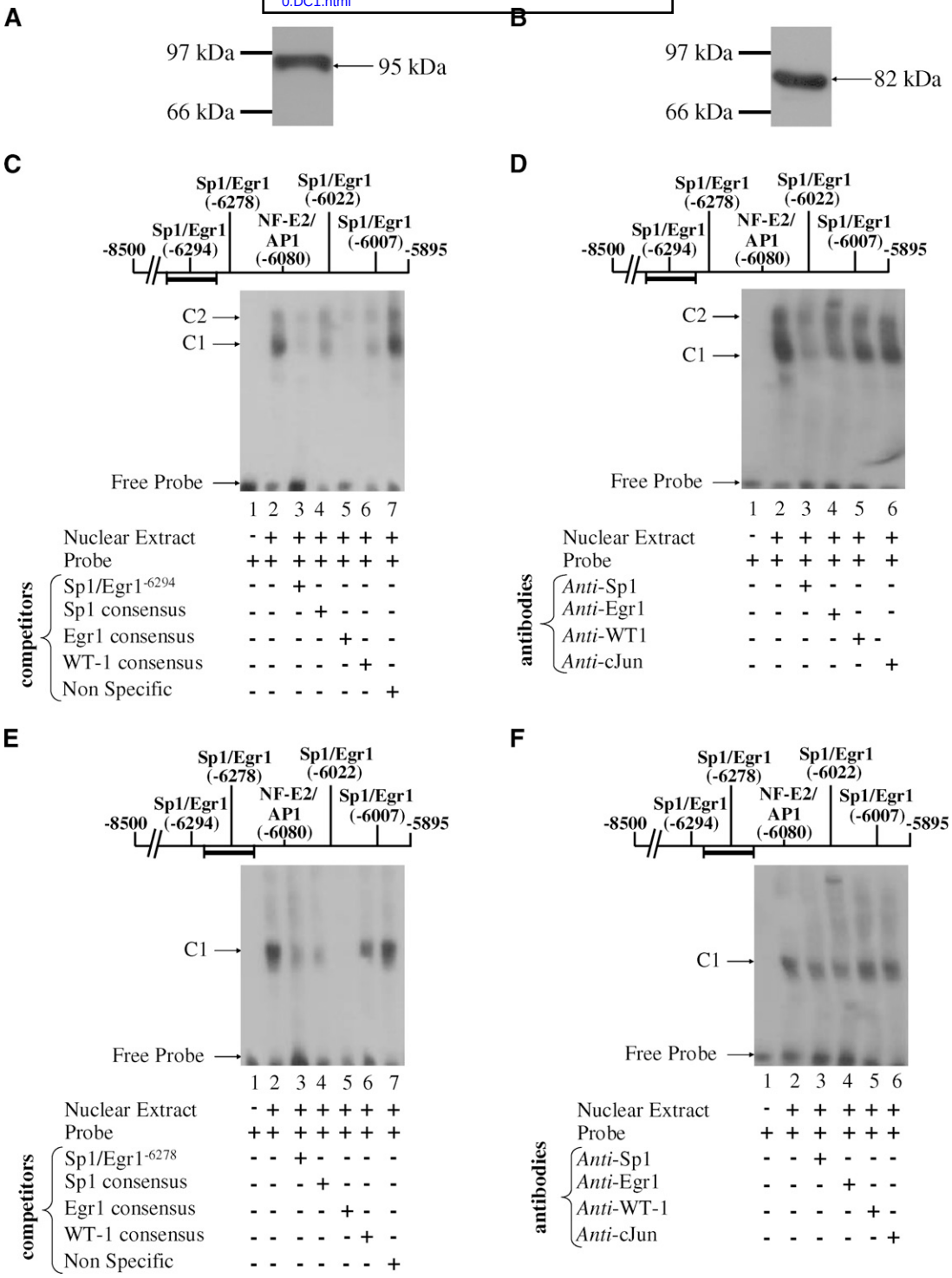

Fig. 4. Nuclear factor binding to overlapping Sp1/Egr1 sites within Prm1. Immunoblot analysis of Sp1 (A) and Egr1 (B) expression in HEL cells (80 μg whole-cell protein/lane). EMSAs (C) or supershift assays (D) using nuclear extract from HEL cells and a biotinylated double-stranded Sp1/Egr1$^{-6,294}$ probe (Probe) spanning −6,299 to −6,276 of the TP gene, as indicated by the horizontal bar. C: Nuclear extract was preincubated with the vehicle (−) or excess nonlabeled competitor oligonucleotides (+) before addition of the Sp1/Egr1$^{-6,294}$ probe. Two main complexes, C1 and C2, were observed. D: Nuclear extract was preincubated with vehicle (−) or with (+) anti-Sp1, anti-Egr1, anti-WT-1, or anti-cJun sera before addition of the Sp1/Egr1$^{-6,294}$ probe. EMSAs (E) or supershift assays (F) using nuclear extract from HEL cells and a biotinylated double-stranded Sp1/Egr1$^{-6,278}$ probe (Probe) spanning −6,283 to −6,255 of the TP gene, as indicated by the horizontal bar. E: Nuclear extract was preincubated with the vehicle (−) or excess nonlabeled competitor oligonucleotides (+) before addition of the Sp1/Egr1^{-6278} probe. One main complex, C1, was observed. F: Nuclear extract was preincubated with vehicle (−) or with (+) anti-Sp1, anti-Egr1, anti-WT-1, or anti-cJun sera before addition of the Sp1/Egr1$^{-6,294}$ probe. Images are representative of three independent experiments.

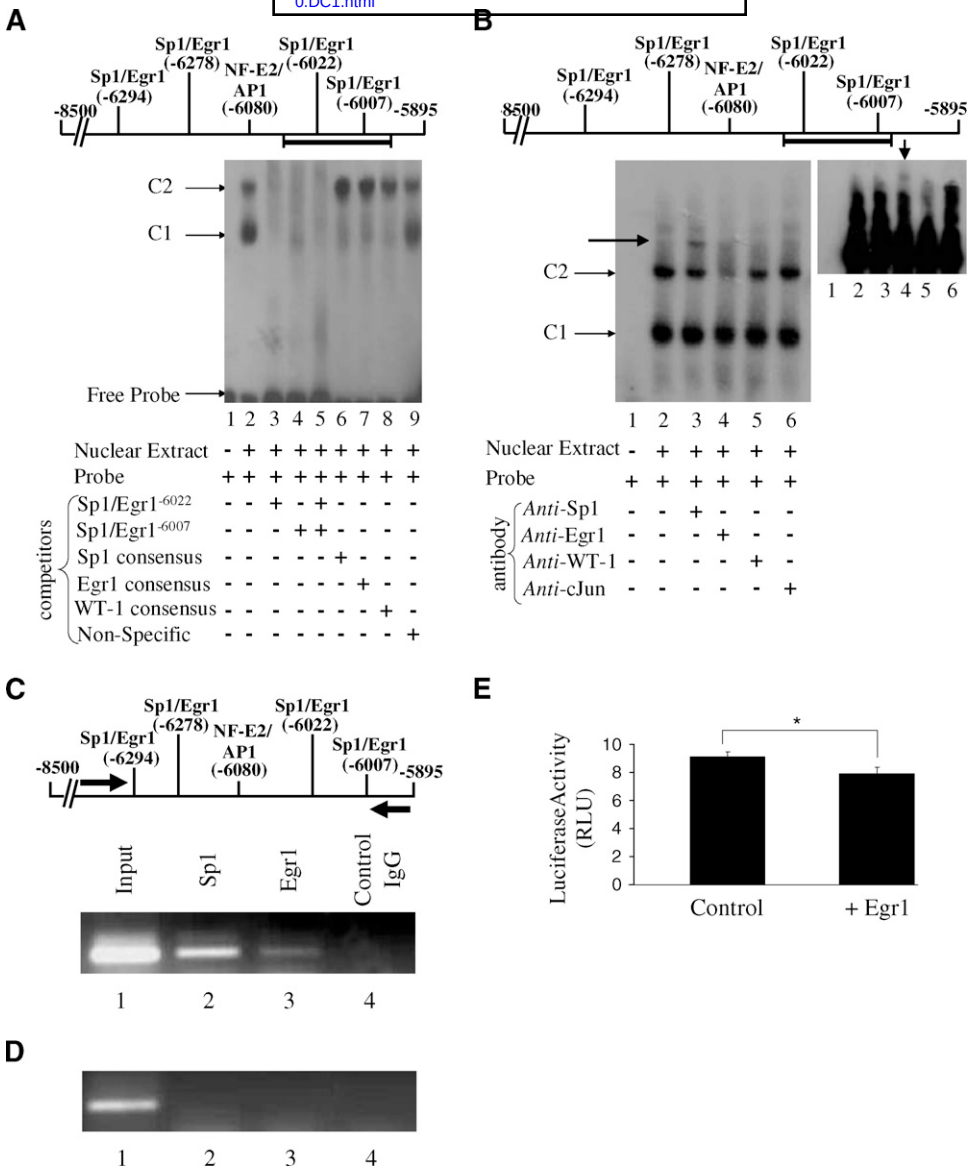

Fig. 5. EMSA and ChIP analysis of Sp1 and Egr1 binding to Prm1. EMSAs (A) or supershift assays (B) using nuclear extract from HEL cells and a biotinylated double-stranded Sp1/Egr1$^{-6,022,-6,007}$ probe (Probe) spanning −6,027 to −5,985 of the TP gene, indicated by the horizontal bar. A: Nuclear extract was preincubated with vehicle (−) or excess nonlabeled competitor oligonucleotides (+) before addition of the Sp1/Egr1$^{-6,022,-6,007}$ probe. Two main complexes, C1 and C2, were observed. B: Nuclear extract was preincubated with vehicle (−) or with (+) anti-Sp1, anti-Egr1, anti-WT-1, or anti-cJun sera before addition of the Sp1/Egr1$^{-6,022,-6,007}$ probe. The image on the right represents a longer exposure of the upper section of the same chromatogram on the left. The arrows indicate the supershifted transcription factor:DNA complex detected with the anti-Sp1 (lane 3, left panel) and anti-Egr1 (lane 4, right panel) sera, respectively. C, D: ChIP analysis of Prm1. Schematic of Prm1 and primers (arrows) used in the PCR to detect the proximal Prm1 region [−6,368 to −5,895; (C)] from input chromatin or immunoprecipitated cross-linked chromatin from HEL cells using anti-Sp1, anti-Egr1, or normal rabbit IgG sera. Primers to detect an upstream region of Prm1 [−8,460 to −8,006; (D)] from input chromatin, anti-Sp1, anti-Egr1, or normal rabbit IgG precipitates were used as a negative control. Images are representative of three independent experiments. E: Effect of overexpression of Egr1 on Prm1-directed gene expression. HEL cells were transiently cotransfected with pGL3b:Prm1HΔ plus pRL-TK in the presence of pCMV-Egr1 (+ Egr1) or with pCMV5 (Control) and expressed as mean relative firefly to renilla luciferase activity (RLU ± SEM; n = 19).

Prm1B$^{GATA(-7,890)*,Ets(-7,870)*}$, where both GATA$^{-7,890}$ and Ets$^{-7,870}$ were mutated, was also significantly lower than that of the wild-type, Prm1B. However, the magnitude of this decrease (2.2-fold) was not greater than that caused by the Ets$^{-7,870}$ mutation alone. Moreover, luciferase activity directed by Prm1B$^{GATA(-7,890)*,Ets(-7,870)*}$ was not significantly different from that directed by Prm1B$^{Ets(-7,870)*}$ ($P = 0.9293$; Fig. 6B). Collectively, these single and combi-

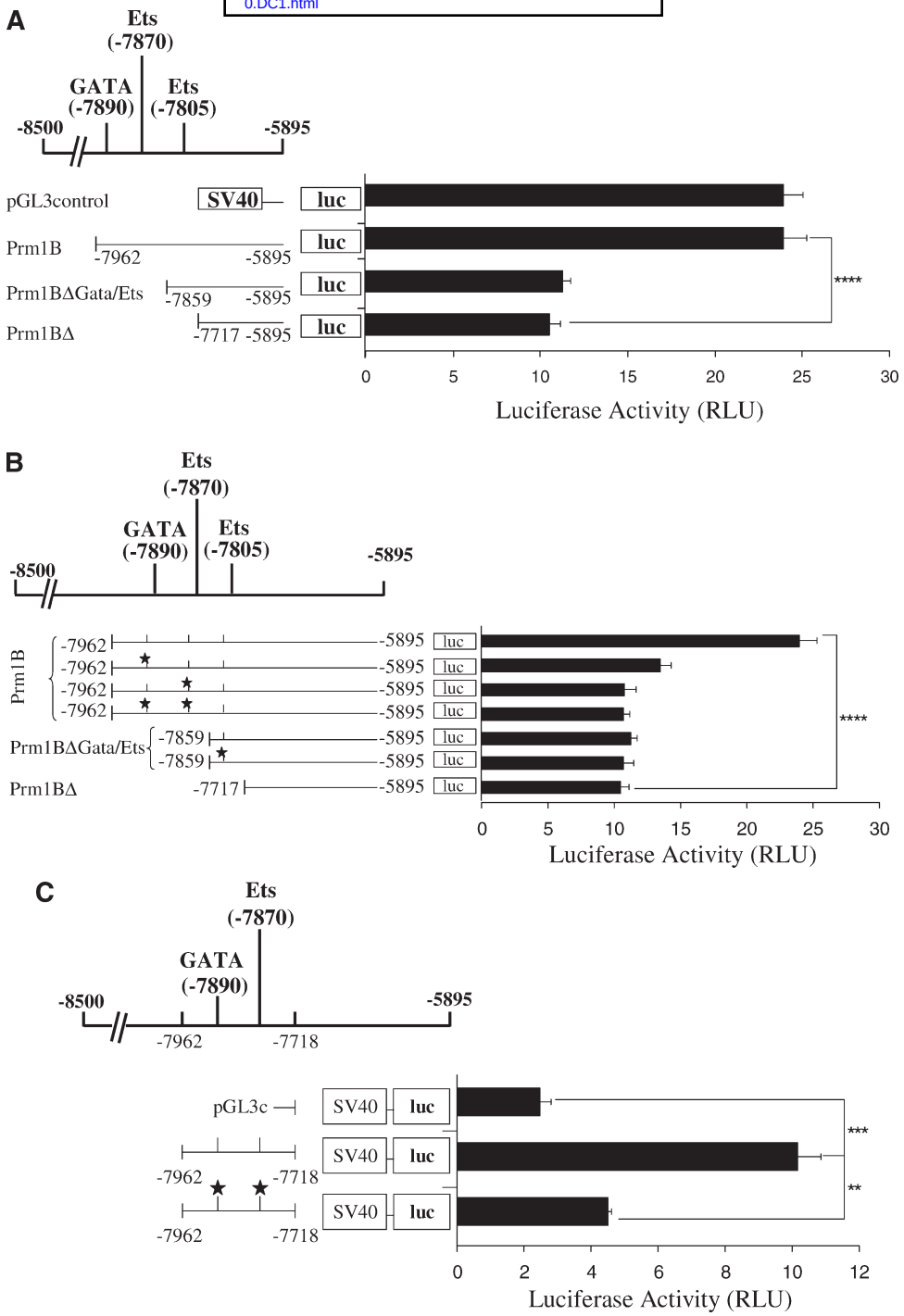

Fig. 6. Identification of functional GATA and Ets elements within Prm1. The positions of putative GATA and Ets elements within Prm1, where the 5′ nucleotide of each element is shown and the star symbol signifies mutated elements. Recombinant pGL3Basic plasmids (2 μg) encoding (A) pGL3control (positive control), Prm1B, Prm1BΔGata/Ets, and Prm1BΔ, or (B) Prm1B, Prm1B$^{GATA(-7,890)*}$, Prm1B$^{Ets(-7,870)*}$, Prm1B$^{GATA(-7,890)*,Ets1(-7,870)*}$, Prm1BΔGata/Ets, Prm1BΔGata/Ets$^{Ets(-7,805)*}$, and Prm1BΔ were cotransfected with pRL-TK into HEL cells. C: A 245 bp subfragment of Prm1, spanning nucleotides −7,962 to −7,718, encoding either the wild-type or mutated (*) GATA$^{(-7,890)}$ and Ets$^{(-7,870)}$ elements was subcloned into pGL3control vector upstream of the SV40 promoter. Resulting recombinant plasmids (0.5 μg), as well as pGL3control (0.5 μg), were cotransfected with pRL-TK into HEL cells. Luciferase activity was expressed as mean firefly relative to renilla luciferase activity (RLU ± SEM; n = 4). Asterisks (*) indicate that the wild-type Prm1 sequence from −7,962 to −7,718 increased luciferase expression directed by pGL3control, while site-directed mutagenesis of the GATA$^{(-7,890)}$ and Ets$^{(-7,870)}$ elements led to decreased luciferase expression compared to that directed by the wild-type sequence.

nation mutations suggest that the GATA$^{-7,890}$ and Ets$^{-7,870}$ elements do not act independently, but rather, cooperatively, in an interdependent manner.

Although, it was already established (Fig. 6A) that there was no difference in luciferase expression directed by Prm1BΔGata/Ets (−7,859) and Prm1BΔ (−7,717), a second putative Ets site, namely Ets$^{-7,805}$, was identified adjacent to the aforementioned GATA$^{-7,890}$ and Ets$^{-7,870}$ sites. However, site-directed mutagenesis of the latter Ets$^{-7,805}$ element did not significantly affect the level of luciferase activity (Fig. 6B; $P = 0.4287$). Hence, collectively these data suggest that GATA$^{-7,890}$ and Ets$^{-7,870}$ elements act as upstream activators of Prm1 and may functionally cooperate to positively regulate basal Prm1 in HEL cells, whereas the putative Ets$^{-7,805}$ element does not appear to be functional.

To investigate the ability of the UAS encoding GATA$^{-7,890}$ and Ets$^{-7,870}$ elements to regulate general gene expression in HEL cells, a Prm1 subfragment spanning −7,962 to −7,718 was placed upstream of the heterologous SV40 promoter in the plasmid pGL3Control. The Prm1GATA/Ets subfragment resulted in a 4.1-fold increase in luciferase expression relative to that of the SV40 promoter alone (Fig. 6C; $P = 0.0003$). Moreover, the level of luciferase expression directed by the Prm1GATA/Ets variant, in which both the GATA$^{-7,890}$ and Ets$^{-7,870}$ elements were mutated, was significantly impaired ($P = 0.0012$), resulting in only a 1.8-fold increase in SV40-directed luciferase activity (Fig. 6C; $P = 0.0003$). These data indicate that the Prm1 region from −7,962 to −7,718 acts as a UAS, greatly increasing the activity of the SV40 promoter in HEL cells, an effect mainly attributable to the GATA$^{-7,890}$ and Ets$^{-7,870}$ *cis*-acting elements.

Thereafter, EMSAs explored the presence of nuclear factors capable of binding to the GATA$^{-7,890}$ and Ets$^{-7,870}$ elements in vitro. Immunoblot analysis confirmed expression of both GATA-1 and Ets-1 in HEL cells (**Fig. 7B, C**). Incubation of a GATA/Ets probe with nuclear extract prepared from HEL cells generated four DNA-protein complexes, C1–C4 (Fig. 7A, lane 2). C2 was competed by either the Prm1 GATA$^{-7,890}$ or Ets$^{-7,870}$ sequences, as well as by a consensus Ets-1, but was not competed by a consensus GATA-1 sequence (Fig. 7A, lane 3–6). These data indicate that C2 consists of Ets-1 and another factor bound to the GATA/Ets probe. C3 was competed by GATA$^{-7,890}$ and consensus GATA-1, but not by Ets$^{-7,870}$ or consensus Ets-1 sequences (Fig. 7A, lanes 3–6, respectively), suggesting that C3 consists of GATA-1 protein, possibly complexed

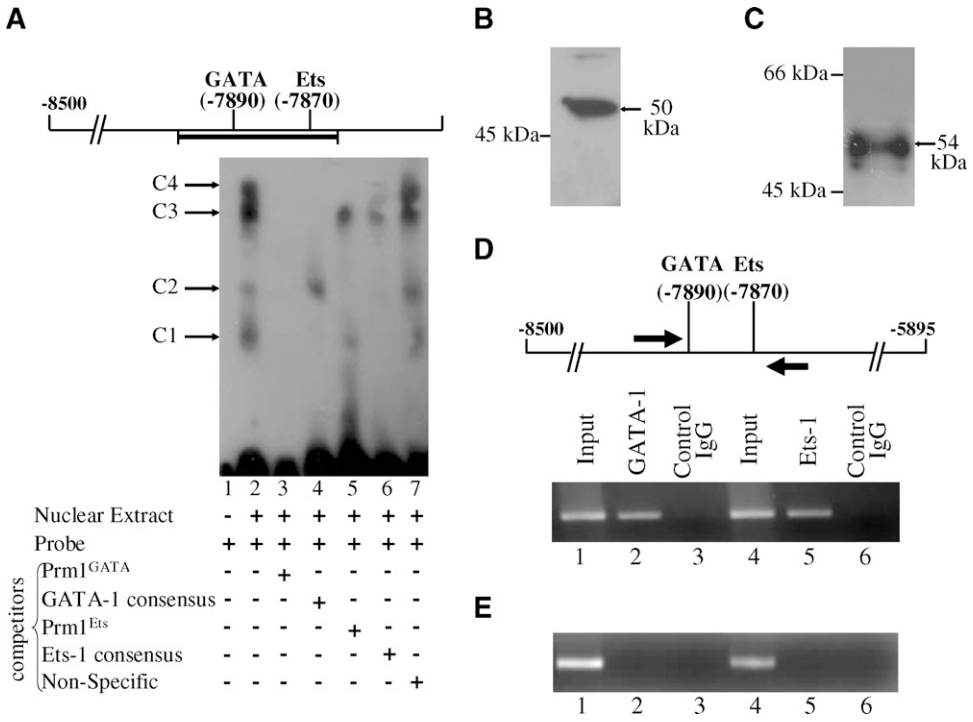

Fig. 7. GATA-1 and Ets-1 binding to Prm1. A: EMSAs using nuclear extract from HEL cells and a biotinylated double-stranded GATA,Ets probe (Probe) spanning −7,890 to −7,848 of the TP gene, indicated by the horizontal bar. Nuclear extract was preincubated with vehicle (−) or excess nonlabeled competitor oligonucleotides (+) before addition of the GATA,Ets probe. Four complexes, C1–C4, were observed. The image is representative of three independent experiments. B, C: Immunoblot analysis of GATA-1 (50 kDa) and Ets-1 (54 kDa) expression in HEL cells (100 μg per lane). D, E: ChIP analysis of Prm1. Schematic of Prm1 and primers (arrows) used in the PCR to detect the Prm1 region from −7,978 to −7,607 (D) from input chromatin, anti-GATA-1, anti-Ets-1, or as a control, normal rabbit IgG immunoprecipitates, as indicated. Primers to detect the proximal Prm1 [−6,368 to −5,895; (D)] from input chromatin, anti-GATA-1, anti-Ets-1, or normal rabbit IgG precipitates were used as a negative control. Images are representative of three independent experiments.

with another factor, bound to the GATA/Ets probe. Complexes C1 and C4 were competed by either $GATA^{-7,890}$ or consensus GATA-1 sequences, as well as by $Ets^{-7,870}$ and consensus Ets-1 sequences (Fig. 7A, lanes 3–6, respectively). The nonspecific competitor, based on a randomized TP gene, failed to inhibit any of the C1–C4 complexes (Fig. 7A, lane 7), confirming the specificity of the GATA/Ets probe. Therefore, complexes of GATA-1 and Ets-1 proteins from HEL cell nuclear extract can bind to Prm1 $GATA^{-7,890}$ and $Ets^{-7,870}$ elements in vitro. Moreover, ChIP assays confirmed the specific amplification of the Prm1 proximal region from anti-GATA-1 and anti-Ets-1 immunoprecipitates, but not from the control IgG precipitate (Fig. 7D), confirming that both GATA-1 and Ets-1 occupy element(s) within the −7,978 to −7,607 region of Prm1 in vivo. Conversely, primers specific to the proximal region of Prm1 from −6,368 to −5,895 resulted in generation of an amplicon from the input chromatin, but not from the GATA-1, Ets-1, or control IgG precipitates (Fig. 7E).

DISCUSSION

In humans, TXA_2 signals through the TPα and TPβ isoforms of its cognate G-protein-coupled receptor. Imbalances in the levels of TXA_2 and TP are implicated in a range of cardiovascular disorders (1–4), but the relative extent to which TPα and TPβ contribute to such pathologies is unknown. Because TPα and TPβ are under the transcriptional control of distinct promoters (18), identification of the factors regulating Prm1 and Prm3 may lead to a greater understanding of their contributory roles in health and disease. Through studies aimed at characterizing Prm3, AP1 and Oct-2 were identified as the key factors regulating its basal activity in HEL cells (19). Moreover, the endogenous cyclopentone 15-deoxy-Δ12,14-prostaglandin J_2 (15d-PGJ_2), a peroxisome proliferator-activated receptor (PPAR)γ ligand, suppressed the transcriptional activity of Prm3 but had no effect on Prm1 (21). Additionally, the synthetic thiazolidinedione (TZD) PPARγ ligands rosiglitazone and troglitazone, used in the treatment of type II diabetes mellitus, selectively suppressed Prm3 activity, without affecting Prm1 (35). An implication of those studies is that the TZD PPARγ ligands may have combined therapeutic benefits in the treatment of type II diabetes and the associated cardiovascular disease, partly due to their suppression of TPβ expression (35).

Prm1 represents the main promoter within the human TP gene (17, 18), but despite this, to date the factors regulating its expression, such as within the vasculature or indeed other tissue/cell types, remain largely undefined. Herein, we sought to identify the key factors regulating basal Prm1 activity in the HEL 92.1.7 megakaryocytic cell line. Prm1 belongs to the class of promoters that lack TATA or CAAT elements. Many TATA-less promoters contain multiple GC-rich elements in their proximal promoter, from which transcription can be activated by the ubiquitously expressed zinc finger transcription factor Sp1 by its recruitment of multi-subunit complex(es) involving $TF_{II}D$ (36). Adjacent Sp1 sites may activate transcription independently from one another, or synergistically through formation of homomultimeric complexes (37). Early growth response protein (Egr)1, another zinc finger transcription factor, also has a GC-rich binding site, and because of the similarity in their consensus elements, adjacent or overlapping sites for Sp1 and Egr1 are frequently found in promoter sequences (38). By mutational analysis and EMSAs, four functional overlapping Sp1/Egr1 elements were identified within the proximal region of Prm1. EMSA and supershift analyses indicated a role for Sp1 and Egr1 binding to each of these elements in vitro, whereas ChIP analysis confirmed the in vivo binding of both endogenous Sp1 and endogenous Egr1 to the proximal Prm1 region of chromatin extracted from HEL cells. Several studies have shown that where overlapping Sp1/Egr1 sites occur in proximal promoter regions, Egr1 negatively regulates Sp1-mediated basal transcription by competitively binding to the overlapping element (38). The four functional Sp1/Egr1 elements identified herein within the proximal Prm1 were adjacent overlapping sites that, through mutational studies, were shown to cooperatively regulate Prm1. Consistent with this, herein, EMSAs confirm that Sp1 and Egr1 generally compete for the same sites within Prm1. Moreover, overexpression of recombinant Egr1 in HEL cells led to a modest but significant reduction in the level of luciferase expression directed by the proximal Prm1. It is likely that overexpression of Egr1 may have led to a more pronounced reduction in Prm1-directed gene expression if the total amount of transfected DNA herein was not limited by the luciferase-based reporter assay itself. Therefore, the combined assessment of these studies suggests that it is likely that Sp1 activates transcription from the TATA-less Prm1 of the TP gene, and that Egr1 negatively regulates this transcription by competing with Sp1 for binding at each of the four overlapping Sp1/Egr1 sites.

In addition to the Sp1/Egr1 sites, we also identified a functional NF-E2/AP1 element by mutational analysis of the proximal Prm1. NF-E2 is a heterodimeric transcription factor that binds to the consensus sequence (T/C)GC*TGA(G/C)TCA*(T/C), with a core AP1 motif (in italics). Although data from EMSA, supershift, and ChIP assays confirmed that endogenous NF-E2 specifically bound to the NF-E2/AP1 element within Prm1 both in vitro and to chromatin in vivo in HEL cells, further studies are necessary to comprehensively investigate the possible binding of AP1 components such as Jun B, Jun D, c-Fos, FosB, Fra1, and Fra2 to the proximal Prm1. The heterodimeric NF-E2 is composed of a tissue-restricted p45 subunit associated with a ubiquitously expressed p18 member of the Maf family (39). Expression of p45 is restricted mainly to hematopoietic progenitors, as well as differentiated erythroid and megakaryocytic cells, mast cells, and granulocytes (40). Originally, it was thought that the primary role of NF-E2 was in erythroid development, owing to its regulation of the porphobilinogen deaminase (40) and globin (41) genes. However, p45-deficient mice exhibited only mild disruption to erythropoiesis but displayed severe thrombocytopenia (<5% of normal platelet count) and high mortality

due to hemorrhage (42). Notable among its megakaryocytic targets, NF-E2 regulates expression of the human (43) and rodent TX synthases (44, 45), platelet-specific Rab27b, β1-tubulin, and caspase-12 (42, 43). Thus, it is suggested that NF-E2 acts as a critical mediator of platelet shedding, regulating a subset of genes involved in late-stage megakaryocyte maturation. Consistent with this, herein, we report that Prm1 of the TP gene is also a bone fide target of NF-E2, suggesting that it plays a critical role in regulating expression of TPα during megakaryocytic differentiation and in platelets in humans. Collectively, although our data have established a role for Sp1, Egr1, and NF-E2 in regulating the core proximal Prm1, they do not exclude the possible involvement of other regulatory elements/factors in this region.

Most eukaryotic promoters contain UASs and URSs. Herein, 5′ deletion analyses revealed two UAS and two URS regions within Prm1. Mutational analysis of the first UAS region (−7,962 to −7,717) identified functional GATA and Ets elements capable of regulating Prm1 and the heterologous SV40 promoter in HEL cells. EMSAs confirmed the presence of nuclear factors in HEL cells capable of binding to the GATA and Ets elements in vitro. Owing to the complex binding patterns of the probe encoding the GATA and Ets elements, supershift assays failed to provide a clear interpretation of the identities of specific transcription factors that bind to these sites in vitro. However, supershift assays were superseded by in vivo ChIP analysis, which confirmed binding of endogenous GATA-1 and endogenous Ets-1 to the Prm1 region of the chromatin in HEL cells. The GATA family of transcription factors are so called because they bind to a consensus A/TGATAA/G DNA sequence. GATA-1 interacts with the coactivator Friend of GATA (FOG)-1 to regulate several genes involved in megakaryocyte differentiation (46). GATA-1 is expressed in hematopoietic progenitor cells, erythrocytes, megakaryocytes, eosinophils, and mast cells and is essential for normal erythropoiesis and megakaryopoiesis (47–49). Loss of megakaryocytic GATA-1 expression in mice resulted in aberrant proliferation and maturation of megakaryocyte cells (50). The Ets family of transcription factors consists of approximately 30 proteins that play a role in a variety of cellular processes such as differentiation, apoptosis, and development. Family members Ets-1, Fli-1, and PU-1 play an important role in megakaryocytic and erythroid differentiation (51). While Ets-1 is downregulated and exported from the nucleus during erythroid maturation, it promotes differentiation and maturation of megakaryocytes (52). ChIP assays have demonstrated that Ets-1 binds to proximal regions in the GPIIb, GPIX, and thrombopoietin receptor (MPL) promoters (53). Moreover, Ets-1 and GATA-1 activate promoters for rat platelet factor 4 (54) and human thrombopoietin receptor, or MPL (55). It is indeed notable that the promoters of these genes are characterized by closely spaced GATA-1 and Ets binding elements, similar to those identified herein in Prm1. Functional cooperativity among GATA-1, FOG-1, and specific Ets family members is required for efficient expression of the megakaryocytic-specific αIIb gene (56). Herein, we report that Prm1 of the human TP gene contains an upstream activator sequence that contains functional elements for GATA and Ets factors separated by 5 bp and that GATA-1 and Ets-1 functionally cooperate by binding to these elements, thereby increasing the expression of TPα in HEL cells. In addition, the ability of a 250 bp subfragment encoding the aforementioned GATA-1 and Ets-1 sites to act as an independent UAS in HEL cells was confirmed whereby it resulted in a 4-fold increase in reporter gene expression directed by the heterologous SV40 promoter.

In conclusion, several critical regulatory regions have been identified within Prm1 of the TP gene, including two UASs and two URSs and a proximal core Prm1 region. Whereas the *trans*-acting factors regulating one of the UASs (−7,717 to −7,504) and the two URS (−8,500 to −7,962 and −6,848 to −6,648) are the subject of ongoing investigations, we have identified four functional overlapping Sp1/Egr1 elements and a single NF-E2 element in the proximal Prm1 region, as well as functional GATA and Ets elements within the UAS, located between −7,962 and −7,859, that regulate basal Prm1 activity. It seems likely that cooperative binding of Sp1 to multiple sites in the proximal Prm1 is an important step required for initiation of transcriptional activity. A similar model has been proposed for regulation of the β-globin gene in erythroleukemia cells, whereby Sp1 binding to multiple sites is required to open the nucleosomal structure, facilitating transcription (57). Herein, it appears that overexpression of Egr1 inhibits the Sp1-mediated activation of Prm1, suggesting that it is the relative balance between Sp1 and Egr1 binding that determines its basal transcription. Additionally, the activity of Prm1 in the HEL megakaryocyte cell line is increased owing to a functional NF-E2 element in the proximal promoter, as well as functional GATA and Ets elements in a UAS. It has been suggested that the hematopoietic-specific factors NF-E2 and GATA-1 stabilize the open nucleosomal structure of the β-globin gene following Sp1 binding (57). Additionally, interactions between Ets factors and Sp1 stabilize Sp1 binding to the αIIb promoter (58). Although further studies are required to elucidate the molecular dynamics of binding, it is likely that the combination of NF-E2, GATA-1, and Ets-1 proteins plays a critical role in regulating Prm1 activity and expression of TPα during different stages of megakaryocytic differentiation and in platelets. Future studies involving overexpression or knockdown of specific factors may, in principle, provide further insight into the regulation of Prm1 and TPα expression. However, owing to the number of factors involved and the various combinations thereof required to complete such an assessment, those experiments are outside the scope of the current study.

The functional characterization of Prm1 herein greatly increases knowledge of the factors regulating expression of the human TP gene. These data not only provide a molecular and genetic basis for understanding the role of TXA_2 and its receptor TP in hemostasis and vascular disease but also provide a rationale for understanding how altered numbers of TPs, such as through dysregulation of signal-

ing by the *trans*-acting factors involved or indeed through genetic polymorphisms in Prm1 itself, contribute to such diseases. Moreover, these data also significantly increase appreciation that expression of the individual TPα and TPβ isoforms, as products of Prm1 and Prm3, respectively, are subject to entirely distinct regulatory mechanisms.

REFERENCES

1. Narumiya, S., Y. Sugimoto, and F. Ushikubi. 1999. Prostanoid receptors: structures, properties, and functions. *Physiol. Rev.* **79:** 1193–1226.
2. Fitzgerald, D. J., L. Roy, F. Catella, and G. A. FitzGerald. 1986. Platelet activation in unstable coronary disease. *N. Engl. J. Med.* **315:** 983–989.
3. Hirsh, P. D., L. D. Hillis, W. B. Campbell, B. G. Firth, and J. T. Willerson. 1981. Release of prostaglandins and thromboxane into the coronary circulation in patients with ischemic heart disease. *N. Engl. J. Med.* **304:** 685–691.
4. Fitzgerald, D. J., W. Rocki, R. Murray, G. Mayo, and G. A. FitzGerald. 1990. Thromboxane A2 synthesis in pregnancy-induced hypertension. *Lancet.* **335:** 751–754.
5. Raychowdhury, M. K., M. Yukawa, L. J. Collins, S. H. McGrail, K. C. Kent, and J. A. Ware. 1994. Alternative splicing produces a divergent cytoplasmic tail in the human endothelial thromboxane A2 receptor. *J. Biol. Chem.* **269:** 19256–19261.
6. Hirata, M., Y. Hayashi, F. Ushikubi, Y. Yokota, R. Kageyama, S. Nakanishi, and S. Narumiya. 1991. Cloning and expression of cDNA for a human thromboxane A2 receptor. *Nature.* **349:** 617–620.
7. Walsh, M., J. F. Foley, and B. T. Kinsella. 2000. Investigation of the role of the carboxyl-terminal tails of the alpha and beta isoforms of the human thromboxane A(2) receptor (TP) in mediating receptor: effector coupling. *Biochim. Biophys. Acta.* **1496:** 164–182.
8. Hirata, T., A. Kakizuka, F. Ushikubi, I. Fuse, M. Okuma, and S. Narumiya. 1994. Arg60 to Leu mutation of the human thromboxane A2 receptor in a dominantly inherited bleeding disorder. *J. Clin. Invest.* **94:** 1662–1667.
9. Vezza, R., A. Habib, and G. A. FitzGerald. 1999. Differential signaling by the thromboxane receptor isoforms via the novel GTP-binding protein, Gh. *J. Biol. Chem.* **274:** 12774–12779.
10. Kelley-Hickie, L. P., and B. T. Kinsella. 2006. Homologous desensitization of signalling by the beta (beta) isoform of the human thromboxane A2 receptor. *Biochim. Biophys. Acta.* **1761:** 1114–1131.
11. Parent, J. L., P. Labrecque, M. Driss Rochdi, and J. L. Benovic. 2001. Role of the differentially spliced carboxyl terminus in thromboxane A2 receptor trafficking: identification of a distinct motif for tonic internalization. *J. Biol. Chem.* **276:** 7079–7085.
12. Reid, H. M., and B. T. Kinsella. 2003. The alpha, but not the beta, isoform of the human thromboxane A2 receptor is a target for nitric oxide-mediated desensitization. Independent modulation of Tp alpha signaling by nitric oxide and prostacyclin. *J. Biol. Chem.* **278:** 51190–51202.
13. Walsh, M. T., J. F. Foley, and B. T. Kinsella. 2000. The alpha, but not the beta, isoform of the human thromboxane A2 receptor is a target for prostacyclin-mediated desensitization. *J. Biol. Chem.* **275:** 20412–20423.
14. Parent, J. L., P. Labrecque, M. J. Orsini, and J. L. Benovic. 1999. Internalization of the TXA2 receptor alpha and beta isoforms. Role of the differentially spliced cooh terminus in agonist-promoted receptor internalization. *J. Biol. Chem.* **274:** 8941–8948.
15. Miggin, S. M., and B. T. Kinsella. 1998. Expression and tissue distribution of the mRNAs encoding the human thromboxane A2 receptor (TP) alpha and beta isoforms. *Biochim. Biophys. Acta.* **1425:** 543–559.
16. Habib, A., G. A. FitzGerald, and J. Maclouf. 1999. Phosphorylation of the thromboxane receptor alpha, the predominant isoform expressed in human platelets. *J. Biol. Chem.* **274:** 2645–2651.
17. Nusing, R. M., M. Hirata, A. Kakizuka, T. Eki, K. Ozawa, and S. Narumiya. 1993. Characterization and chromosomal mapping of the human thromboxane A2 receptor gene. *J. Biol. Chem.* **268:** 25253–25259.
18. Coyle, A. T., S. M. Miggin, and B. T. Kinsella. 2002. Characterization of the 5′ untranslated region of alpha and beta isoforms of the human thromboxane A2 receptor (TP). Differential promoter utilization by the TP isoforms. *Eur. J. Biochem.* **269:** 4058–4073.
19. Coyle, A. T., and B. T. Kinsella. 2005. Characterization of promoter 3 of the human thromboxane A receptor gene. A functional AP-1 and octamer motif are required for basal promoter activity. *FEBS J.* **272:** 1036–1053.
20. D'Angelo, D. D., M. G. Davis, W. A. Houser, J. J. Eubank, M. E. Ritchie, and G. W. Dorn II. 1995. Characterization of 5′ end of human thromboxane receptor gene. Organizational analysis and mapping of protein kinase C-responsive elements regulating expression in platelets. *Circ. Res.* **77:** 466–474.
21. Coyle, A. T., M. B. O'Keeffe, and B. T. Kinsella. 2005. 15-Deoxy delta 12,14-prostaglandin J2 suppresses transcription by promoter 3 of the human thromboxane A2 receptor gene through peroxisome proliferator-activated receptor gamma in human erythroleukemia cells. *FEBS J.* **272:** 4754–4773.
22. Saffak, T., and R. M. Nusing. 2002. The 5′ region of the human thromboxane A(2) receptor gene. *Prostaglandins Leukot. Essent. Fatty Acids.* **67:** 25–31.
23. Hoffmann, E., J. Ashouri, S. Wolter, A. Doerrie, O. Dittrich-Breiholz, H. Schneider, E. F. Wagner, J. Troppmair, N. Mackman, and M. Kracht. 2008. Transcriptional regulation of EGR-1 by the interleukin-1-JNK-MKK7-c-Jun pathway. *J. Biol. Chem.* **283:** 12120–12128.
24. Kooren, J., R. J. Palstra, P. Klous, E. Splinter, M. von Lindern, F. Grosveld, and W. de Laat. 2007. Beta-globin active chromatin Hub formation in differentiating erythroid cells and in p45 NF-E2 knockout mice. *J. Biol. Chem.* **282:** 16544–16552.
25. Murakami, Y., S. Yamagoe, K. Noguchi, Y. Takebe, N. Takahashi, Y. Uehara, and H. Fukazawa. 2006. Ets-1-dependent expression of vascular endothelial growth factor receptors is activated by latency-associated nuclear antigen of Kaposi's sarcoma-associated herpes virus through interaction with Daxx. *J. Biol. Chem.* **281:** 28113–28121.
26. Sawado, T., K. Igarashi, and M. Groudine. 2001. Activation of beta-major globin gene transcription is associated with recruitment of NF-E2 to the beta-globin LCR and gene promoter. *Proc. Natl. Acad. Sci. USA.* **98:** 10226–10231.
27. Sinha-Datta, U., I. Horikawa, E. Michishita, A. Datta, J. C. Sigler-Nicot, M. Brown, M. Kazanji, J. C. Barrett, and C. Nicot. 2004. Transcriptional activation of hTERT through the NF-kappaB pathway in HTLV-I-transformed cells. *Blood.* **104:** 2523–2531.
28. Sobue, S., K. Hagiwara, Y. Banno, K. Tamiya-Koizumi, M. Suzuki, A. Takagi, T. Kojima, H. Asano, Y. Nozawa, and T. Murate. 2005. Transcription factor specificity protein 1 (Sp1) is the main regulator of nerve growth factor-induced sphingosine kinase 1 gene expression of the rat pheochromocytoma cell line, PC12. *J. Neurochem.* **95:** 940–949.
29. Sohn, R. H., C. B. Deming, D. C. Johns, H. C. Champion, C. Bian, K. Gardner, and J. J. Rade. 2005. Regulation of endothelial thrombomodulin expression by inflammatory cytokines is mediated by activation of nuclear factor-kappa B. *Blood.* **105:** 3910–3917.
30. Zhang, F., T. E. Ahlborn, C. Li, F. B. Kraemer, and J. Liu. 2002. Identification of Egr1 as the oncostatin M-induced transcription activator that binds to sterol-independent regulatory element of human LDL receptor promoter. *J. Lipid Res.* **43:** 1477–1485.
31. Thiel, G., S. Schoch, and D. Petersohn. 1994. Regulation of synapsin I gene expression by the zinc finger transcription factor zif268/egr-1. *J. Biol. Chem.* **269:** 15294–15301.
32. Quandt, K., K. Frech, H. Karas, E. Wingender, and T. Werner. 1995. MatInd and MatInspector: new fast and versatile tools for detection of consensus matches in nucleotide sequence data. *Nucleic Acids Res.* **23:** 4878–4884.
33. Azizkhan, J. C., D. E. Jensen, A. J. Pierce, and M. Wade. 1993. Transcription from TATA-less promoters: dihydrofolate reductase as a model. *Crit. Rev. Eukaryot. Gene Expr.* **3:** 229–254.
34. Koch, C. M., R. M. Andrews, P. Flicek, S. C. Dillon, U. Karaoz, G. K. Clelland, S. Wilcox, D. M. Beare, J. C. Fowler, P. Couttet, et al. 2007. The landscape of histone modifications across 1% of the human genome in five human cell lines. *Genome Res.* **17:** 691–707.
35. Coyle, A. T., and B. T. Kinsella. 2006. Synthetic peroxisome proliferator-activated receptor gamma agonists rosiglitazone and troglitazone suppress transcription by promoter 3 of the human thromboxane A2 receptor gene in human erythroleukemia cells. *Biochem. Pharmacol.* **71:** 1308–1323.
36. Pugh, B. F., and R. Tjian. 1991. Transcription from a TATA-less promoter requires a multisubunit TFIID complex. *Genes Dev.* **5:** 1935–1945.
37. Pascal, E., and R. Tjian. 1991. Different activation domains of Sp1 govern formation of multimers and mediate transcriptional synergism. *Genes Dev.* **5:** 1646–1656.
38. Huang, R. P., Y. Fan, Z. Ni, D. Mercola, and E. D. Adamson. 1997.

Reciprocal modulation between Sp1 and Egr-1. *J. Cell. Biochem.* **66:** 489–499.
39. Andrews, N. C., K. J. Kotkow, P. A. Ney, H. Erdjument-Bromage, P. Tempst, and S. H. Orkin. 1993. The ubiquitous subunit of erythroid transcription factor NF-E2 is a small basic-leucine zipper protein related to the v-maf oncogene. *Proc. Natl. Acad. Sci. USA.* **90:** 11488–11492.
40. Mignotte, V., L. Wall, E. deBoer, F. Grosveld, and P. H. Romeo. 1989. Two tissue-specific factors bind the erythroid promoter of the human porphobilinogen deaminase gene. *Nucleic Acids Res.* **17:** 37–54.
41. Kotkow, K. J., and S. H. Orkin. 1995. Dependence of globin gene expression in mouse erythroleukemia cells on the NF-E2 heterodimer. *Mol. Cell. Biol.* **15:** 4640–4647.
42. Shivdasani, R. A., M. F. Rosenblatt, D. Zucker-Franklin, C. W. Jackson, P. Hunt, C. J. Saris, and S. H. Orkin. 1995. Transcription factor NF-E2 is required for platelet formation independent of the actions of thrombopoietin/MGDF in megakaryocyte development. *Cell.* **81:** 695–704.
43. Deveaux, S., S. Cohen-Kaminsky, R. A. Shivdasani, N. C. Andrews, A. Filipe, I. Kuzniak, S. H. Orkin, P. H. Romeo, and V. Mignotte. 1997. p45 NF-E2 regulates expression of thromboxane synthase in megakaryocytes. *EMBO J.* **16:** 5654–5661.
44. Ikeda, Y., A. Sugawara, Y. Taniyama, A. Uruno, K. Igarashi, S. Arima, S. Ito, and K. Takeuchi. 2000. Suppression of rat thromboxane synthase gene transcription by peroxisome proliferator-activated receptor gamma in macrophages via an interaction with NRF2. *J. Biol. Chem.* **275:** 33142–33150.
45. Zhang, L., H. Xiao, R. A. Schultz, and R. F. Shen. 1997. Genomic organization, chromosomal localization, and expression of the murine thromboxane synthase gene. *Genomics.* **45:** 519–528.
46. Nichols, K. E., J. D. Crispino, M. Poncz, J. G. White, S. H. Orkin, J. M. Maris, and M. J. Weiss. 2000. Familial dyserythropoietic anaemia and thrombocytopenia due to an inherited mutation in GATA1. *Nat. Genet.* **24:** 266–270.
47. Harigae, H. 2006. GATA transcription factors and hematological diseases. *Tohoku J. Exp. Med.* **210:** 1–9.
48. Patient, R. K., and J. D. McGhee. 2002. The GATA family (vertebrates and invertebrates). *Curr. Opin. Genet. Dev.* **12:** 416–422.
49. Szalai, G., A. C. LaRue, and D. K. Watson. 2006. Molecular mechanisms of megakaryopoiesis. *Cell. Mol. Life Sci.* **63:** 2460–2476.
50. Shivdasani, R. A., Y. Fujiwara, M. A. McDevitt, and S. H. Orkin. 1997. A lineage-selective knockout establishes the critical role of transcription factor GATA-1 in megakaryocyte growth and platelet development. *EMBO J.* **16:** 3965–3973.
51. Oikawa, T., and T. Yamada. 2003. Molecular biology of the Ets family of transcription factors. *Gene.* **303:** 11–34.
52. Lulli, V., P. Romania, O. Morsilli, M. Gabbianelli, A. Pagliuca, S. Mazzeo, U. Testa, C. Peschle, and G. Marziali. 2006. Overexpression of Ets-1 in human hematopoietic progenitor cells blocks erythroid and promotes megakaryocytic differentiation. *Cell Death Differ.* **13:** 1064–1074.
53. Jackers, P., G. Szalai, O. Moussa, and D. K. Watson. 2004. Ets-dependent regulation of target gene expression during megakaryopoiesis. *J. Biol. Chem.* **279:** 52183–52190.
54. Minami, T., K. Tachibana, T. Imanishi, and T. Doi. 1998. Both Ets-1 and GATA-1 are essential for positive regulation of platelet factor 4 gene expression. *Eur. J. Biochem.* **258:** 879–889.
55. Deveaux, S., A. Filipe, V. Lemarchandel, J. Ghysdael, P. H. Romeo, and V. Mignotte. 1996. Analysis of the thrombopoietin receptor (MPL) promoter implicates GATA and Ets proteins in the coregulation of megakaryocyte-specific genes. *Blood.* **87:** 4678–4685.
56. Wang, X., J. D. Crispino, D. L. Letting, M. Nakazawa, M. Poncz, and G. A. Blobel. 2002. Control of megakaryocyte-specific gene expression by GATA-1 and FOG-1: role of Ets transcription factors. *EMBO J.* **21:** 5225–5234.
57. Goodwin, A. J., J. M. McInerney, M. A. Glander, O. Pomerantz, and C. H. Lowrey. 2001. In vivo formation of a human beta-globin locus control region core element requires binding sites for multiple factors including GATA-1, NF-E2, erythroid Kruppel-like factor, and Sp1. *J. Biol. Chem.* **276:** 26883–26892.
58. Block, K. L., Y. Shou, and M. Poncz. 1996. An Ets/Sp1 interaction in the 5′-flanking region of the megakaryocyte-specific alpha IIb gene appears to stabilize Sp1 binding and is essential for expression of this TATA-less gene. *Blood.* **88:** 2071–2080.